Folate pathway modulation in *Rhipicephalus* ticks in response to infection

Filipa Dias* (1), Joana Couto*ǂ (2), Joana Ferrolho (2), Gustavo S. Seron (2), Lesley Bell-Sakyi (3), Sandra Antunes (2), Ana Domingos (2)

(1) Departamento de Biologia, Universidade de Aveiro, Campus Universitário de Santiago, 3810-193 Aveiro, Portugal; (2) Global Health and Tropical Medicine, Instituto de Higiene e Medicina Tropical, Universidade Nova de Lisboa (GHTM-IHMT-UNL), Rua da Junqueira 100, 1349-008 Lisboa, Portugal; (3) Department of Infection Biology, Institute of Infection and Global Health, University of Liverpool, Liverpool, L3 5RF, United Kingdom

*These authors contributed equally to this work.

ǂCorresponding author: Joana Couto, E-mail: jmanuel.couto@ihmt.unl.pt

Summary:

Folate pathways components were demonstrated to be present in RNA-sequencing data obtained from uninfected and pathogen-infected *Rhipicephalus* ticks. Here, PCR and qPCR allowed the identification of folate-related genes in *Rhipicephalus* spp. ticks and in the tick cell line IDE8. Genes coding for GTP cyclohydrolase I (*gch-I*), thymidylate synthase (*ts*) and 6-pyrovoyltetrahydropterin (*ptps*) were identified. Differential gene expression was evaluated by qPCR between uninfected and infected samples of four biological systems, showing significant upregulation and largest fold-change for the *gch-I* gene in the majority of the biological systems, supporting the selection for functional analysis by RNAi silencing. Efficient knockdown of the *gch-I* gene in uninfected and *Ehrlichia canis*-infected IDE8 cells showed no detectable impact on the capacity of the bacteria to invade or replicate in the tick cells. Overall, this work demonstrated an increase in the expression of some folate-related genes, though not always statistically significantly, in the presence of infection, suggesting gene expression modulation of these pathways, either as a tick response to an invader or manipulation of the tick cell machinery by the

pathogens to their advantage. This discovery points to folate pathways as interesting targets for further studies.

Keywords

Folate; RNAi; Tick-borne diseases; Tick cell line; Vector-pathogen interface

Introduction

Tick-borne diseases (TBDs) are responsible for a great burden on human and animal health worldwide (Jongejan & Uilenberg, 2004). With the increase in emerging TBDs observed in recent decades (Wikel, 2018), there is an urgent need for the development of cost-effective and environmentally-friendly strategies for tick control and transmission-blocking alternatives (Mapholi et al., 2014). The development of transmission-blocking strategies with the capacity to affect several pathogens across multiple tick species is economically and technically attractive. Such an accomplishment could only be attained by pinpointing key vector pathways. However, the key step for the design of such approaches relies on the selection of promising targets with important biological roles, which can be hampered by the lack of tick genomic resources. RNA-sequencing projects are a useful resource for the selection of targets in "non-model" organisms (Oppenheim, Baker, Simon, & DeSalle, 2015).

Folate pathway components were present in RNA-sequencing data obtained from *Rhipicephalus* spp. ticks (*Rhipicephalus bursa* - Antunes et al., 2018, *Rhipicephalus annulatus* - Antunes et al., 2019 and *Rhipicephalus sanguineus* – BioProject: PRJNA362595) that are important vectors of causative agents of diseases of farm animals and pets such as *Babesia ovis*, *Babesia bigemina* and *Ehrlichia canis* (Sonenshine & Roe, 2014). Folate-related compounds and enzymes are essential in a vast panoply of physiological processes, having a broad impact on cell growth and in the normal development of organisms (Ducker & Rabinowitz, 2017). This study aims to identify and evaluate the expression profile of folate-related genes, and to further assess by gene knockdown the role of a selected target in cell survival and infection. Here, we applied PCR and qPCR for the identification and assessment of expression patterns of three genes from these pathways, coding

for GTP cyclohydrolase I (GCH-I), thymidylate synthase (TS) and 6-pyruvoyltetrahydropterin synthase (PTPS), in *Rhipicephalus* ticks and in the tick cell line IDE8. Genes *gch-I* and *ptps* code for the enzymes of the first two steps of production of tetrahydrobiopterin (BH4), an essential cofactor for the production of nitric oxide (NO) and amine neurotransmissors (Werner, Blau, & Thöny, 2011). TS is responsible for the production of thymidine (dTMP) and therefore involved in DNA replication and cell multiplication (Ackland, Clarke, Beale, & Peters, 2006). Differential expression of these genes during infection was analyzed in four biological systems: *R. annulatus* – *B. bigemina*; *R. bursa* – *B. ovis*; *R. sanguineus* – *E. canis*; IDE8 cells – *E. canis*, allowing the selection of candidate genes for further functional analysis by RNA interference (RNAi) *in vitro* (Barry et al., 2013). Studies focusing on folate-related pathways will contribute to a deeper understanding of their role in the vector-host interface.

Materials and Methods

Samples: RNA from individual salivary glands (SGs) was obtained from: seven uninfected and seven *B. ovis*-infected *R. bursa* ticks, as described by Antunes et al., (2018); ten uninfected and ten *B. bigemina*-infected *R. annulatus* ticks, as described by Antunes et al., (2012); and three uninfected and three-*E. canis* infected pools containing ten pairs of SGs each from the tropical lineage of *R. sanguineus* ticks, as described by Ferrolho et al. (2017). Only female ticks were used. All ticks were fully engorged except *R. sanguineus* which were freshly-molted adults. The *Ixodes scapularis* embryo-derived cell line IDE8 (Munderloh, Liu, Wang, Chen, & Kurtti, 1994) was maintained in two conditions: uninfected and infected with semipurified *E. canis*, Spain 105 strain (Zweygarth et al., 2014) following the protocol described by Ferrolho et al. (2016) except that 0.1% $NaHCO_3$ and 10 mM HEPES were not added to the culture medium. RNA was extracted using Tri-Reagent (Sigma–Aldrich, St. Louis, MO, USA), the quality and integrity of all RNA samples was evaluated using the QIAxcel equipment and kit (Qiagen, Hilden, Germany) according to the manufacturer's instructions, and concentrations were estimated by ND-1000 Spectrophotometer (NanoDrop ND1000, Thermo Fisher Scientific, Whaltman, MA, USA). RNA

concentrations of 500 ng/µL for *R. annulatus* and IDE8, 250 ng/µL for *R. sanguineus* and 150 ng/µL for *R. bursa* were used for cDNA synthesis with iScript™ cDNA Synthesis Kit (Bio-Rad, Hercules, CA, USA) in a T100 Thermal Cycler (Bio-Rad).

Gene identification: PCR was performed with NZYTaq II 2× Green Master Mix (NZYTech, Lisboa, Portugal) in a total reaction volume of 25 µL following the manufacturer's protocol in a T100 Thermal Cycler (Bio-Rad). qPCR was performed in triplicate using the iTaq™ Universal SYBR® Green Supermix (Bio-Rad) and a total reaction volume of 10 µL in a CFX96 Touch Real-time PCR (Bio-Rad). For qPCR a standard curve with serial dilutions was included to determine amplification efficiency through the standard curve slope. Primer sequences and conditions are listed in Table 1. Products were purified with NZYGelpure kit (NZYTech, Lisboa, Portugal) and sequenced by the Sanger method (StabVida, Caparica, Portugal). InterPro (available at www.ebi.ac.uk/interpro/) was used to check the presence in the identified sequences of conserved domains including active sites.

Differential expression analysis: Differential gene expression between uninfected and infected samples was carried out by qPCR. The expression of four candidate reference genes, 16S rDNA (Ferrolho et al., 2017), *β-tubulin, β-actin* and *elf* (Nijhof, Balk, Postigo, & Jongejan, 2009) was evaluated in each biological system using the *geNorm* algorithm (Vandesompele et al., 2002) incorporated in the CFX Manager™ Software (Bio-Rad). Data normalization was performed using the reference genes that showed the lowest variation: 16S rDNA, *β-tubulin, β-actin* and *elf* for *R. annulatus*; 16S rDNA, *β-tubulin* and *elf* for *R. bursa*; *β-actin* and *elf* for *R. sanguineus*; 16S rDNA, *β-tubulin* and *β-actin* for IDE8 cells. .Relative gene expression after normalization was assessed using the above-mentioned software by the $^{\Delta\Delta}$Cq (Livak & Schmittgen, 2001) and Pfaff (Pfaff, 2001) methods. Outliers were singled out by the Tukey method (Tukey, 1977) and Cq-values were compared between conditions by Student's *t* test. A statistically-significant difference was considered when the *p*-value was less than 0.05.

RNA interference: Specific primers containing a T7 promoter sequence in the 5´ end (Fw: 5'-ACGACGAGATGGTCATTGTG-3' and Rv: 5'-AGCGTCGTGTCCCACTCTT-3') were used to amplify by PCR a fragment of 461 bp of the *gch-I* gene with iProof™ High Fidelity DNA Polymerase (Bio-Rad, USA). This product was used for double-stranded RNA (dsRNA) synthesis using the MEGAscript RNAi Kit (Ambion, Austin, TX, USA). For the *in vitro* silencing assay, cells were seeded in 24-well plates and 24 hours later *gch-I* dsRNA or dsRNA for an unrelated control gene, mouse *beta-2 microglobulin* (*β2m*) (Couto et al., 2017), was added at a concentration of $5x10^{10}$ molecules/µL. The assay included three groups: Group A - uninfected IDE8 cells; Group B – uninfected IDE8 cells that were inoculated with *E. canis* 24 hours after dsRNA addition (to evaluate the effect on bacterial invasion); Group C - IDE8 cells with a 7-day pre-established *E. canis* infection (to evaluate the effect on bacterial multiplication). Three time points were evaluated: 24 h (T1), 96 h (T2) and 144 h (T3) after dsRNA addition. Giemsa-stained cytocentrifuge smears (Ferrolho et al., 2016) were also performed for morphological analysis. Five replicates were collected for RNA extraction and 250 ng/µL were used for cDNA synthesis. qPCR analysis of *gch-I* expression was performed as described above and data was normalized with 16S rDNA, *β-actin*, and *r13a* (Weisheit et al., 2015). qPCR was also applied for relative quantification of *E. canis* with the ehrlichial *dsb* gene (Doyle et al., 2005), using cDNA as template, and data was normalized against *β-actin* and *r13a*.Percentage of gene silencing was calculated as the ratio of *gch-I* expression between the treated group (exposed to *gch-I* dsRNA) and the control group (exposed to *β2m* dsRNA).

Results and Discussion

PCR and qPCR allowed the amplification of three genes: *gch-I*, *ts* and *ptps* in *R. annulatus*, *R. bursa*, *R. sanguineus* and the IDE8 cell line, that showed identities between 71% and 99 % with the mRNA sequences originally retrieved from different ixodid species (Table 1) and, as such, were considered to correspond to folate pathway-related genes. Conserved domains containing active sites were identified in these sequences. The *gch-I* sequences presented the two conserved active sites from GTP cyclohydrolase I (IPR018234), while *ptps* sequences showed the cysteine

(IPR022470) and the histidine (IPR022469) active site from the 6-pyruvoyl tetrahydropterin synthase. The *ts* sequences from *Ixodes* spp. exhibited the active site from thymidylate synthase (IPR020940). Differential expression of those genes, after infection, was evaluated in four biological systems: *R. annulatus* – *B. bigemina*; *R. bursa* – *B. ovis*; *R. sanguineus* – *E. canis*; IDE8 – *E. canis* (Fig. 1). The non-vector tick cell line IDE8 was used because it supports continuous growth of *E. canis*, in contrast to cell lines derived from the vector *R. sanguineus* (Ferrolho et al., 2016). For the *gch-I* gene, statistically-significant up-regulation ($p < 0.05$) was observed for infected samples of *R. annulatus* ($p < 0.001$; 4.8-fold change), *R. bursa* ($p = 0,002$; 3.3-fold change) and in IDE8 cells ($p < 0.001$; 2.7- fold change). In *R. sanguineus*, however, there was no difference in gene expression between uninfected and *E. canis*-infected ticks. For the *ts* gene, samples from *Rhipicephalus* spp. ticks showed an increase in expression when the pathogen was present, being 2.2-fold change for *R. annulatus* ($p = 0.129$), 1.3-fold change for *R. bursa* ($p = 0.072$) and 1.6-fold change for *R. sanguineus* ($p = 0.428$), although these changes were not significant; for the IDE8 cell line there was no difference in expression between uninfected and *E. canis*-infected samples ($p = 0.634$). For the *ptps* gene, statistically-significant up-regulation was observed in *R. annulatus* ($p = 0.007$; 1.7-fold change) and *R. bursa* ($p < 0.001$; 1.3-fold change) when *Babesia* was present. *R. sanguineus* showed an increase in expression ($p = 0.158$; 1.7-fold change) and the IDE8 cell line had a slight decrease ($p = 0.237$; 0.8-fold change) in the presence of *E. canis*. The proteins encoded by the *gch-I* and *ptps* genes are responsible for *de novo* biosynthesis of BH4, an essential cofactor for the synthesis of NO. In mice, treatment with lipopolysaccharides was proven to stimulate the production of NO by increasing BH4 levels, while treatment with 4-Diamino-6-hydroxypyrimidine, a GCH-I inhibitor, led to the reduction of NO levels (Gross & Levi, 1992). As such, exposure to infectious pathogens may be responsible for the increased expression of these genes, as an immune defense mechanism by the tick. The *ts* gene is involved in the production of nucleotides having an important role in cell replication events, and is a target in cancer therapy (Chu, Callender, Farrell, & Schmitz, 2003); however its role in the tick-pathogen interface is unclear. Overall, we observed a tendency for up-regulation of these genes in the presence of the pathogens suggesting gene expression modulation, either as

an auto-protective tick reaction to the invader microorganisms or as subversion of the vector machinery by the pathogens to their advantage in a similar manner to that observed in *Anaplasma phagocytophilum*. This pathogen has been shown to manipulate expression of proteins such as spectrin alpha chain and mitochondrial porins, involved in cytoskeleton rearrangement and mitochondrial induced apoptosis respectively, to subvert host cell defense (Ayllón et al., 2013).

Gene *gch-I* was selected for an *in vitro* silencing assay, with silencing efficiency ranging from 83.2% to 100% between experimental groups. A significant increase in *dsb* gene expression was observed between time points for Groups B and C, demonstrating typical *E. canis* multiplication within cells. Relative levels of *E. canis dsb* expression (Fig. 2) were not significantly different between the infected IDE8 cell groups exposed to *gch-I* and *β2m* dsRNA for any of the conditions ($p > 0.05$). Examination of the Giemsa-stained cytocentrifuge smears did not reveal striking differences in morphological characteristics of the tick cell line or the bacteria in the presence of *gch-I* dsRNA. Silencing of the *gch-I* gene did not affect the capacity of *E. canis* to infect and replicate in the tick cells. However, further studies, such as validation of protein under-representation and enzyme inhibition assays, are needed to clarify the silencing results and to explore the function of the encoded protein. Also, since BH4 can be acquired by salvage pathway, new studies are needed in order to evaluate the role of dihydrofolate reductase in the replenishment of BH4 pools in ticks, through inhibition of the biopterin salvage pathway, a mechanism well described in vertebrates (Crabtree, Tatham, Hale, Alp, & Channon, 2009). The tick microbiome may also play a role in the bioavailability of BH4. A study on GCH-I deficient mice showed that some endosymbiotic bacteria, belonging to the phylum Actinobacteria, have the capacity to produce this compound (Belik et al., 2017). This phylum could also supply BH4 in ticks since those bacteria were shown to be the second most represented in microbiomes of *Amblyomma maculatum* (Varela-Stokes et al., 2018) and *Ixodes ricinus* (Carpi et al., 2011). Moreover, BH4 could also be provided through carrier proteins in cell membranes present in ticks (Perner et al., 2016) which are responsible for the uptake of folate derivates, due to their shared biopterin ring structure (Frye, 2013). Therefore, the effects of *gch-I* knockdown might be undetectable in a short-time frame, hiding potential effects on tick cell fitness and in the

interaction with *E. canis*. The performance of assays with an extended time frame would help to understand the importance of this enzyme in the tick-pathogen interaction.

Conclusions

Here we observed an overall overexpression of three genes from the folate pathways in ticks, *gch-I*, *ts* and *ptps*, which although not always statistically significant in infected ticks and/or cells, suggests gene modulation caused by the presence of the parasite. Although silencing of the *gch-I* gene did not influence the capacity of *E. canis* to infect and replicate in the IDE8 cell line over a short time-frame, this study showed that genes from the folate pathways are interesting targets for further studies on the vector-pathogen interface. *In vitro* assays with folate analogs capable of enzymatic inhibition, taking into consideration both vector and pathogen enzymatic machinery, would help elucidate their role in tick cells and in interaction with pathogens.

Acknowledgements

This work was supported by Fundação para a Ciência e a Tecnologia (FCT) under the projects TICKVAC (PTDC/CVT-WEL/1807/2014) and TICKOMIC (PTDC/CVT-CVT/29073/2017). Authors would like to acknowledge FCT for funds to GHTM - UID/Multi/04413/2013. SA is the recipient of a post-doctoral grant supported by FCT (SFRH/BPD/108957/2015) and JC and JF are the recipients of Ph.D. grants supported by the FCT (SFRH/BD/121946/2016, SFRH/BD/122894/2016, respectively). L B-S is supported by the United Kingdom Biotechnology and Biological Sciences Research Council (grant number BB/P024270/1). The tick cell line IDE8 was provided by the Tick Cell Biobank, and was used by kind permission of Prof. Ulrike Munderloh, University of Minnesota. The *E. canis* (Spain 105) was used with permission of Dr Erich Zweygarth.

Conflict of Interest

The authors declare that there are no conflicts of interest regarding the publication of this article.

References

Ackland, S. P., Clarke, S. J., Beale, P., & Peters, G. J. (2006). Thymidylate synthase inhibitors. *Update on Cancer Therapeutics*, *1*(4), 403–427. https://doi.org/10.1016/J.UCT.2006.09.001

Antunes, S., Couto, J., Ferrolho, J., Rodrigues, F., Nobre, J., Santos, A. S., … Domingos, A. (2018). *Rhipicephalus bursa* sialotranscriptomic response to blood feeding and *Babesia ovis* infection: Identification of candidate protective antigens. *Frontiers in Cellular and Infection Microbiology*, *8*(116), 1–17. https://doi.org/10.3389/fcimb.2018.00116

Antunes, S., Couto, J., Ferrolho, J., Sanches, G. S., Merino Charrez, J. O., De la Cruz Hernández, N., … Domingos, A. (2019). Transcriptome and Proteome Response of *Rhipicephalus annulatus* Tick Vector to *Babesia bigemina* Infection. *Frontiers in Physiology*, *10*, 318. https://doi.org/10.3389/fphys.2019.00318

Antunes, S., Galindo, R. C., Almazán, C., Rudenko, N., Golovchenko, M., Grubhoffer, L., … Domingos, A. (2012). Functional genomics studies of *Rhipicephalus* (*Boophilus*) *annulatus* ticks in response to infection with the cattle protozoan parasite, *Babesia bigemina*. *International Journal for Parasitology*, *42*(2), 187–195. https://doi.org/10.1016/J.IJPARA.2011.12.003

Ayllón, N., Villar, M., Busby, A. T., Kocan, K. M., Blouin, E. F., Bonzón-Kulichenko, E., … de la Fuente, J. (2013). *Anaplasma phagocytophilum* inhibits apoptosis and promotes cytoskeleton rearrangement for infection of tick cells. *Infection and Immunity*, *81*(7), 2415–25. https://doi.org/10.1128/IAI.00194-13

Barry, G., Alberdi, P., Schnettler, E., Weisheit, S., Kohl, A., Fazakerley, J. K., & Bell-Sakyi, L. (2013). Gene silencing in tick cell lines using small interfering or long double-stranded RNA. *Experimental & Applied Acarology*, *59*(3), 319–38. https://doi.org/10.1007/s10493-

012-9598-x

Belik, J., Shifrin, Y., Arning, E., Bottiglieri, T., Pan, J., Daigneault, M. C., & Allen-Vercoe, E. (2017). Intestinal microbiota as a tetrahydrobiopterin exogenous source in hph-1 mice. *Scientific Reports*, *7*, 39854. https://doi.org/10.1038/srep39854

Carpi, G., Cagnacci, F., Wittekindt, N. E., Zhao, F., Qi, J., Tomsho, L. P., … Schuster, S. C. (2011). Metagenomic Profile of the Bacterial Communities Associated with *Ixodes ricinus* Ticks. *PLoS ONE*, *6*(10), e25604. https://doi.org/10.1371/journal.pone.0025604

Chu, E., Callender, M. A., Farrell, M. P., & Schmitz, J. C. (2003). Thymidylate synthase inhibitors as anticancer agents: from bench to bedside. *Cancer Chemotherapy and Pharmacology*, *52*(0), 80–89. https://doi.org/10.1007/s00280-003-0625-9

Couto, J., Antunes, S., Pinheiro-Silva, R., Do Rosário, V., De La Fuente, J., & Domingos, A. (2017). Solute carriers affect *Anopheles stephensi* survival and *Plasmodium berghei* infection in the salivary glands. *Scientific Reports*, *7*(1). https://doi.org/10.1038/s41598-017-06317-6

Crabtree, M. J., Tatham, A. L., Hale, A. B., Alp, N. J., & Channon, K. M. (2009). Critical Role for Tetrahydrobiopterin Recycling by Dihydrofolate Reductase in Regulation of Endothelial Nitric-oxide Synthase Coupling. *Journal of Biological Chemistry*, *284*(41), 28128–28136. https://doi.org/10.1074/jbc.M109.041483

Doyle, C. K., Labruna, M. B., Breitschwerdt, E. B., Tang, Y.-W., Corstvet, R. E., Hegarty, B. C., … McBride, J. W. (2005). Detection of medically important *Ehrlichia* by quantitative multicolor TaqMan real-time polymerase chain reaction of the *dsb* gene. *The Journal of Molecular Diagnostics : JMD*, *7*(4), 504–10. https://doi.org/10.1016/S1525-1578(10)60581-8

Ducker, G. S., & Rabinowitz, J. D. (2017). One-Carbon Metabolism in Health and Disease. *Cell Metabolism*, *25*(1), 27–42. https://doi.org/10.1016/j.cmet.2016.08.009

Ferrolho, J., Antunes, S., Sanches, G. S., Couto, J., Évora, P. M., Rosa, C., … Domingos, A. (2017). *Ferritin 1* silencing effect in *Rhipicephalus sanguineus* sensu lato (Acari: Ixodidae) during experimental infection with *Ehrlichia canis*. *Ticks and Tick-Borne Diseases*, *8*(1). https://doi.org/10.1016/j.ttbdis.2016.10.015

Ferrolho, J., Simpson, J., Hawes, P., Zweygarth, E., & Bell-Sakyi, L. (2016). Growth of *Ehrlichia canis*, the causative agent of canine monocytic ehrlichiosis, in vector and non-vector ixodid tick cell lines. *Ticks and Tick-Borne Diseases*, *7*(4), 631–637. https://doi.org/10.1016/j.ttbdis.2016.01.013

Frye, R. E. (2013). Tetrahydrobiopterin May Be Transported into the Central Nervous System by the Folate R eceptor α, *6*(3), 117–120. https://doi.org/10.7156/najms.2013.0603117

Gross, S. S., & Levi, R. (1992). Tetrahydrobiopterin synthesis. An absolute requirement for cytokine-induced nitric oxide generation by vascular smooth muscle. *The Journal of Biological Chemistry*, *267*(36), 25722–9.

Jongejan, F., & Uilenberg, G. (2004). The global importance of ticks. *Parasitology*, *129 Suppl*, S3-14. Retrieved from http://www.ncbi.nlm.nih.gov/pubmed/15938502

Livak, K., & Schmittgen, T. (2001). Analysis of relative gene expression data using real-time quantitative PCR and the 2− ΔΔCT method. *Methods*, *25*(4), 402–408. https://doi.org/10.1006/meth.2001.1262

Mapholi, N. O., Marufu, M. C., Maiwashe, A., Banga, C. B., Muchenje, V., MacNeil, M. D., … Dzama, K. (2014). Towards a genomics approach to tick (Acari: Ixodidae) control in cattle: A review. *Ticks and Tick-Borne Diseases*, *5*(5), 475–483. https://doi.org/10.1016/j.ttbdis.2014.04.006

Munderloh, U. G., Liu, Y., Wang, M., Chen, C., & Kurtti, T. J. (1994). Establishment, maintenance and description of cell lines from the tick *Ixodes scapularis*. *The Journal of Parasitology*, *80*(4), 533–43. https://doi.org/10.2307/3283188

290 Nijhof, A. M., Balk, J. A., Postigo, M., & Jongejan, F. (2009). Selection of reference genes for
291 quantitative RT-PCR studies in *Rhipicephalus* (*Boophilus*) *microplus* and *Rhipicephalus*
292 *appendiculatus* ticks and determination of the expression profile of Bm86. *BMC Molecular*
293 *Biology*, *10*(1), 112. https://doi.org/10.1186/1471-2199-10-112

294 Oppenheim, S. J., Baker, R. H., Simon, S., & DeSalle, R. (2015). We can't all be supermodels:
295 the value of comparative transcriptomics to the study of non-model insects. *Insect Molecular*
296 *Biology*, *24*(2), 139–54. https://doi.org/10.1111/imb.12154

297 Perner, J., Provazník, J., Schrenková, J., Urbanová, V., Ribeiro, J. M. C., & Kopáček, P. (2016).
298 RNA-seq analyses of the midgut from blood- and serum-fed *Ixodes ricinus* ticks. *Scientific*
299 *Reports*, *6*(June), 1–18. https://doi.org/10.1038/srep36695

300 Pfaff, M. W. (2001). A new mathematical model for relative quantification in real-time RT-PCR.
301 *Nucleic Acids Research*, *29*(9), e45. https://doi.org/10.1093/NAR/29.9.E45

302 Sonenshine, D. E., & Roe, R. M. (2014). *Biology of ticks* (2nd ed.). New York: Oxford University
303 Press.

304 Tukey, J. (1977). *Exploratory data analysis*. Retrieved from http://theta.edu.pl/wp-
305 content/uploads/2012/10/exploratorydataanalysis_tukey.pdf

306 Vandesompele, J., De Preter, K., Pattyn, F., Poppe, B., Van Roy, N., De Paepe, A., & Speleman,
307 F. (2002). Accurate normalization of real-time quantitative RT-PCR data by geometric
308 averaging of multiple internal control genes. *Genome Biology*, *3*(7), research0034.1–
309 research0034.11. Retrieved from http://www.ncbi.nlm.nih.gov/pubmed/12184808

310 Varela-Stokes, A. S., Park, S. H., Stokes, J. V., Gavron, N. A., Lee, S. I., Moraru, G. M., & Ricke,
311 S. C. (2018). Tick microbial communities within enriched extracts of *Amblyomma*
312 *maculatum*. *Ticks and Tick-Borne Diseases*, *9*(4), 798–805.
313 https://doi.org/10.1016/j.ttbdis.2018.02.022

314 Weisheit, S., Villar, M., Tykalová, H., Popara, M., Loecherbach, J., Watson, M., … Bell-Sakyi,

L. (2015). *Ixodes scapularis* and *Ixodes ricinus* tick cell lines respond to infection with tick-borne encephalitis virus: transcriptomic and proteomic analysis. *Parasites & Vectors*, *8*(1), 599. https://doi.org/10.1186/s13071-015-1210-x

Werner, E. R., Blau, N., & Thöny, B. (2011). Tetrahydrobiopterin: biochemistry and pathophysiology. *Biochemical Journal*, *438*(3), 397–414. https://doi.org/10.1042/BJ20110293

Wikel, S. (2018). Ticks and Tick-Borne Infections: Complex Ecology, Agents, and Host Interactions. *Veterinary Sciences*, *5*(2), 60. https://doi.org/10.3390/vetsci5020060

Zweygarth, E., Cabezas-Cruz, A., Josemans, A. I., Oosthuizen, M. C., Matjila, P. T., Lis, K., … Passos, L. M. F. (2014). *In vitro* culture and structural differences in the major immunoreactive protein gp36 of geographically distant *Ehrlichia canis* isolates. *Ticks and Tick-Borne Diseases*, *5*(4), 423–431. https://doi.org/10.1016/j.ttbdis.2014.01.011

Figure 1 - Differential gene expression in four different tick-pathogen biological systems. Relative expression of *gch-I* (A), *ts* (B) and *ptps* (C) genes for the infected (INF) samples compared with the non-infected (NI) controls in the four biological systems: *Rhipicephalus annulatus - Babesia bigemina*, *Rhipicephalus bursa – Babesia ovis*, *Rhipicephalus sanguineus - Ehrlichia canis;* IDE8 – *E. canis*. The graphs represent the mean ± SEM with statistically-significant differences indicated with $p < 0.01$ (**), $p < 0.001$ (***).

Figure 2 - Relative normalized expression of *Ehrlichia canis dsb* over time in infected IDE8 cells. Relative expression of the *dsb* gene for samples of group B - uninfected IDE8 cells inoculated with *E. canis* 24 h after addition of the dsRNA, and group C - IDE8 cells already infected with *E. canis*. Samples were exposed to:dsRNA for *β2m* (grey triangles), dsRNA for

gch-I (black spheres) or medium alone (grey squares). Analysis was carried out at three time points: 24 hours (T1), 96 hours (T2) and 144 hours (T3). Points in the graph represent the means (n = 5), and error bars represent the corresponding standard deviation. Statistically-significant differences ($p < 0.05$) between time points calculated with the Mann-Whitney test for each treatment are indicated with asterisks (*) above the black bar for *gch-I* samples and the grey bar for control *β2m* samples.

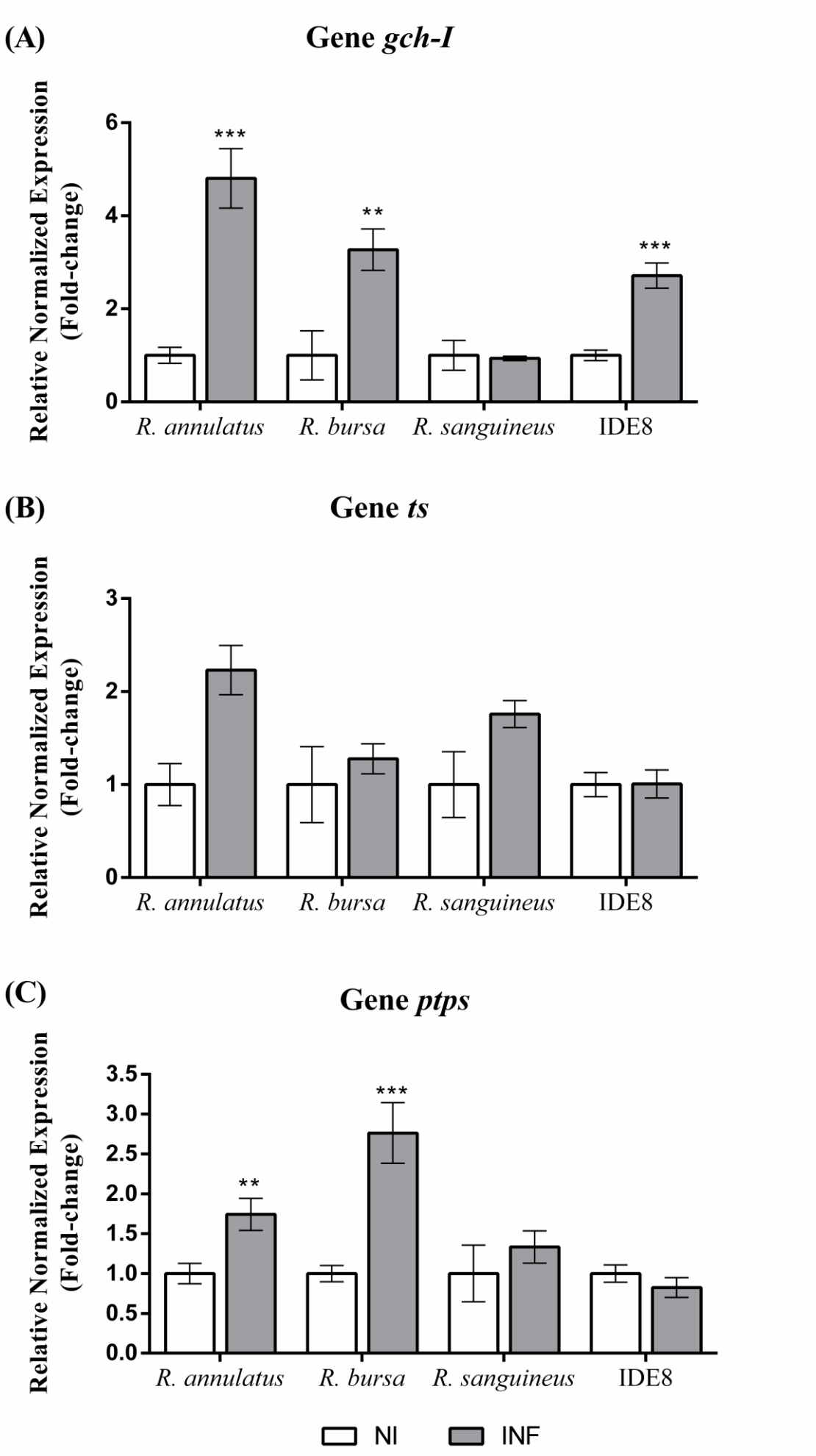
(A)
Gene gch-I
Relative Normalized Expression (Fold-change)
6
4
2
0
***
**
***
R. annulatus
R. bursa
R. sanguineus
IDE8
(B)
Gene ts
Relative Normalized Expression (Fold-change)
3
2
1
0
R. annulatus
R. bursa
R. sanguineus
IDE8
(C)
Gene ptps
Relative Normalized Expression (Fold-change)
3.5
3.0
2.5
2.0
1.5
1.0
0.5
0.0
**
***
R. annulatus
R. bursa
R. sanguineus
IDE8
NI
INF

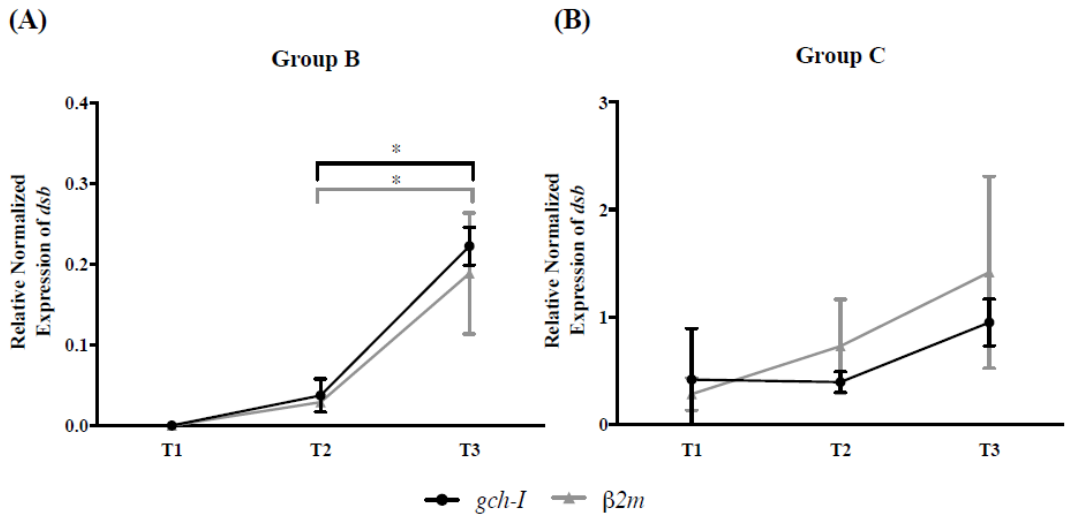
(A)
Group B
Relative Normalized Expression of dsb
0.4
0.3
0.2
0.1
0.0
*
*
T1
T2
T3
(B)
Group C
Relative Normalized Expression of dsb
3
2
1
0
T1
T2
T3
gch-I
β2m

348

349

Supplementary File

Folate pathway modulation in *Rhipicephalus* ticks in response to infection

Filipa Dias* (1), Joana Couto*ǂ (2), Joana Ferrolho (2), Gustavo S. Seron (2), Lesley Bell-Sakyi (3), Sandra Antunes (2), Ana Domingos (2)

(1) Departamento de Biologia, Universidade de Aveiro, Campus Universitário de Santiago, 3810-193 Aveiro, Portugal; (2) Global Health and Tropical Medicine, Instituto de Higiene e Medicina Tropical, Universidade Nova de Lisboa (GHTM-IHMT-UNL), Rua da Junqueira 100, 1349-008 Lisboa, Portugal; (3) Department of Infection Biology, Institute of Infection and Global Health, University of Liverpool, Liverpool, L3 5RF, United Kingdom

*These authors contributed equally to this work.

ǂCorresponding author: Joana Couto, E-mail: jmanuel.couto@ihmt.unl.pt

Putative Genes	Accession number	Primer Forward and Reverse (5'-3')	Species	Primer Concentration (µM)	Annealing Temperature (C°)
gch-I	XM_002410022.1† (IS)	GTCAACGATGCYGTGTTC	*Rhipicephalus spp.* and *I. scapularis*	0,5	60
		GCTTGKATSACMACTCCGAC			
ptps	JO841409.1 † (AM)	ACGCGGATTGAATCMTTCAG	*Rhipicephalus spp.*	0,5	60
		TTCTTGTGATCAAGRGCATCC			
	JAB68508.1 (IR)	AGCAGCATACAGCGTCAGG	*I. scapularis*	0,5	58
		TCTCGTGAAGCCGAACTTGG			
ts	XM_002410017.1 † JAA56783.1 (IS, RP)	TATGGATTYCAGTGGAGGC	*I. scapularis*	0,5	59
		ACRTAGAACTGYGCYARG			
	JAA56783.1 (RP)	ACAGACCCACGATGAATACC	*Rhipicephalus spp.*	0,5	54
		CCGTAGACCCTCTTAGAAACC			

Supplementary Table 1 – Primer sequences with corresponding Accession Numbers. Primer concentration and annealing temperatures are listed for *Rhipicephalus* spp. (*Rhipicephalus*

365 *annulatus*, *Rhipicephalus bursa*, *Rhipicephalus sanguineus*) and *Ixodes scapularis*. The tick
366 species origins of the sequences are indicated below the Accession Numbers (IS – *I. scapularis;*
367 AM - *Amblyomma maculatum;* IR – *Ixodes ricinus;* RP – *Rhipicephalus pulchellus*).

368

369

370

371 † Primer designed by alignment of corresponding mRNA sequence and its transcriptomic
372 sequences, for each gene.

373

374